Journal of Medical Imaging

Journal of Medical Imaging

Journal of Medical Imaging

OPEN ACCESS

_____

Magnetic Nanoclusters for T2 MR Imaging in Cancer using Xenograft Mice Model

[1]Jooyeon Kim, [2]GilJae Lee, [3]Jingyu Kim*

Abstract In this study, we tried to develop nanoprobe for molecular magnetic resonance (MR) imaging using magnetic nanoclusters (MNC). MNCs for magnetic resonance imaging were synthesized by thermal decomposition.

The size of the synthesized MNC was confirmed to be 73 ± 32.4 nm. Cytotoxicity test of the synthesized MNCs showed that the cell state of about 80% or more did not change in all the treatment ranges and cell survival rate was high even though the MNCs were injected. MNC was injected intravenously into the tail vein of nude mice.

[1]Jooyeon Kim e-mail : jooyun8992@kbsi.re.kr
Department of Research Equipment Operation
Korea Basic Science Institute, Cheong-won, Ochang, Republic of Korea

[2]GilJae Lee* (✉)   ***corresponding author***
Business Promotion Agency, Chungbuk Technopark (28116)40, Yeongudanji-ro, Cheongju-si, Chungcheongbuk-do, Korea

[3]Jingyu Kim
Dept. of Radiological & Madico-Oncological Science, University of Science & Technology
(34113) 217, Gajeong-ro, Yuseong-gu, Daejeon, Korea
e-mail : jingyu8754@kirams.re.kr

As a result, it was found that enhancement of the contrast was confirmed in xenograft mice model using MNC. These results will contribute to clinical application and related research through magnetic nanocluster in the future.

1. INTRODUCTION

Molecular imaging is a technique for diagnosing various changes at the cellular level. It is a field where advanced imaging technology and molecular cell biology are combined and has recently developed rapidly through a fusion of medicine, genetics, molecular biology, cytology, chemistry, pharmacology, physics, biomedical engineering, radiology, and nuclear medicine.

The imaging technologies and devices used in molecular imaging are Single Photon Emission Computed Tomography (SPECT), Positron Emission Tomography (PET), Magnetic Resonance Imaging (MRI), Ultrasonography, Fluorescence, and Bioluminescence. Molecular imaging has used for early diagnosis of cancer, new drug development,

gene therapy, stem cell research and treatment, and disease prognosis prediction[1]. MR molecular imaging can be performed noninvasively without radiation exposure. In addition, MR molecular imaging has excellent safety and image quality. Recently, chemical exchange saturation transfer (CEST), magnetic nanoparticles (MNPs) and magnetic nano clusters (MNCs) Research are being actively carried out.

MNCs are structures in which nanoparticles of 1 to 100 nanometers (10 to - 9 meters) in diameters, such as MNPs, gold nanoparticles, and quantum dots, are assembled. This structure has unique collective properties that are different from single nanoparticles. The MNCs showed a T_2 relaxation rate three times higher than that of the conventional MR imaging contrast agent Feridex and was well transferred to specific cells.

These results demonstrate that MNPs can be used in biomedical and medical applications such as MR molecular imaging, fluorescence imaging, and drug delivery [2].

This study is to develop a novel nanoprobe for MR molecular imaging of gastric cancer using MNCs based on MNPs which can be used for MR molecular imaging.

2. EXPERIMENTAL METHODS

2.1. Materials

Polysorbate, ethylenediamine, 1,4-dioxane, 4-dimethylamino-pyridine, triethylamine, and succinic anhydride(SA) were purchased from Sigma Aldrich Chemical Co. Phosphate buffered saline (PBS: 10 mM, pH 7.4) were purchased from Roswell Park Memorial Institute, and antibiotic-antimycotic solution Dialysis membrane was used. The gastric cancer cell line (American type culture collection) was incubated in an incubator containing fetal bovine serum and antibiotic antimycotic. Ultra pure deionized water was used for all synthesis.

2.2. Synthesis of Magnetic Nano Cluster

MNC was synthesized by the nanoemulsion method. The nanoemulsion process was carried out by following the two-step synthetic procedure. First, monocrystalline manganese iron nanoparticles are synthesized by pyrolysis from non-polar inorganic solvent to metal-inorganic precursors, and synthesized manganese iron is synthesized by seed-mediated growth method.

2.3. MNC Cytotoxicity Test

The gastric cancer cell line was cultured under the conditions of RPMI medium and antibiotics, and various concentrations of MNCs were treated for 4 hours. The cytotoxicity test of MNC on gastric cancer cell line was performed by measuring 3- (4,5-dimethyl-thiazole-2-yl) -2,5-diphenyltetrazolium bromide (MTT) assay.

2.4 Zenograft animal models and experimental procedures

All animal studies were approved and accredited by the Association for Assessment and Accreditation of Laboratory Animal Care (AAALAC) International. Six-week-old female nude mice were injected intravenously with an anesthetic Zolethyl / Rompun mixture. After anesthesia, 1.0×10^7 gastric cancer cell lines were dispersed in 200 mL saline solution and injected into the thighs of mice. MR images were obtained at 5th week after transplantation of gastric cancer cell line.

2.3 MR Imaging

Animal solution MRI was performed with 3 T Phillips clinical MRI equipment and T_2 weighted images were obtained using wrist coils. The conditions for obtaining T_2-weighted images were TR (repetition time): 700.85 ms, TE (echo time: 100.65 ms), Slice thickness: 1.0 mm, and FOV read: 100 mm.

3. RESULT & DISCUSSION

3.1. MNCs Characteristics

MNCs for MR contrast agents were synthesized by thermal decomposition methods. The manganese iron in the inorganic state was combined with PLI (Poly-L-Lysine) by emulsion method, and the remaining PLI was removed using Centrifuge and MNCs were synthesized with proper PLI ratio. As shown in [Figure 1], transmission electron microscope (TEM) was used to confirm the size distribution and morphology of MNCs. TEM confirmed that the size of the MNCs was 73 ± 32.4 nm.

(1) MNP   (2) MNC
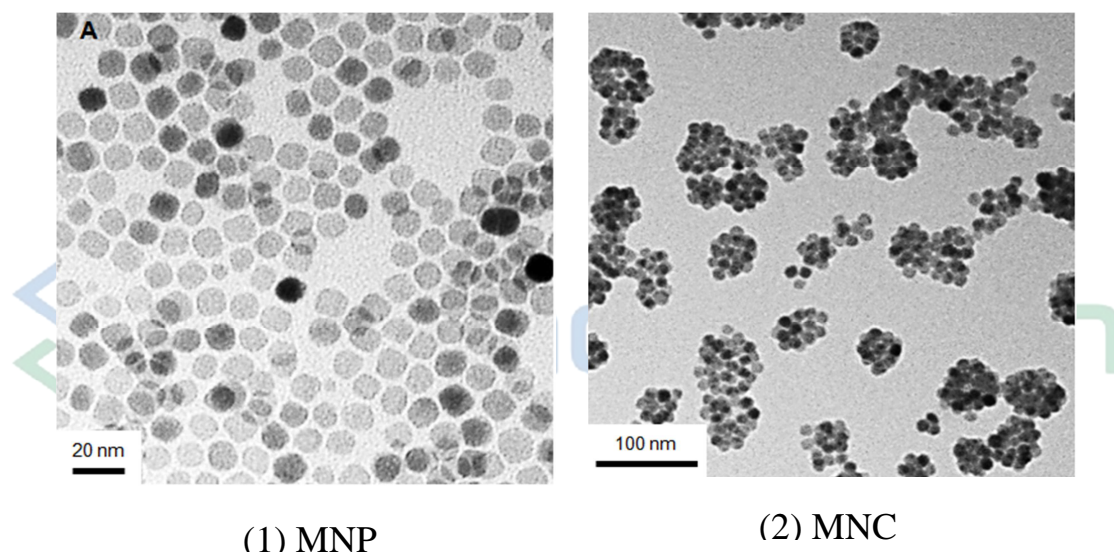
[Figure 1] TEM imaging of MNP and MNC

MRI was performed to confirm the characteristics of the synthesized cluster as a MRI contrast agent. Appropriate-sized clusters could adequately avoid the reticuloendothelial system (RES), allowing them to stay longer in the blood.

As shown in [Figure 2], T_2 images according to cluster concentration were confirmed through MRI, and it was confirmed that the T_2 value was increased with increasing concentration as shown in [Figure 3].
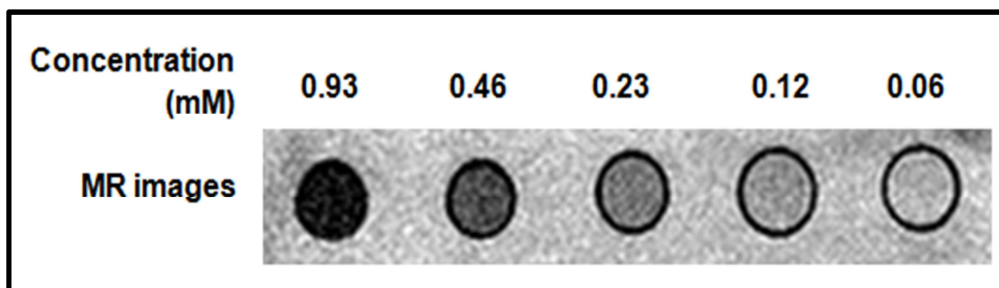
[Figure 2] MNCs T2 imaging
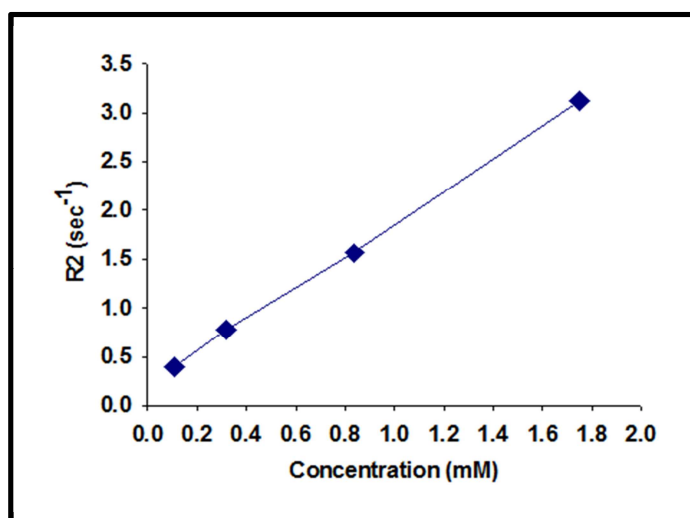
[Figure 3] R_2 relaxation rate with increasing MNCs concentration

3.2. MNC cytotoxicity test

Cytotoxicity tests should be carried out to determine the side effects of drugs intended to be injected into the living body including the contrast agent. Although there are objections to the sacrifice of animals, experiments through simulations have not been fully validated to date. Animal experiments are performed to reproduce the target concentration changes and effects of experimental cell lines during ADME (administration, distribution, metabolism, and emission) processes and processes in vivo with high accuracy.

In this study, cell growth retardation was examined using animal experimental cell lines. We investigated normal cell damage and normal cell function after injection of MNCs contrast agent.

To evaluate cytotoxicity, 3-(4,5-dimethylthiazol-2-yl) -2,5-diphenyltetrazolium bromide (MTT) test was performed on gastric cancer cell line. The gastric cancer cell line was treated with NMCs synthesized in the range of 10^{-7} to 10^{-1} and cultured for 24 hours.[Figure 4] shows the appearance of particle-type MNPs contrast agent and clustered MNCs contrast agent.
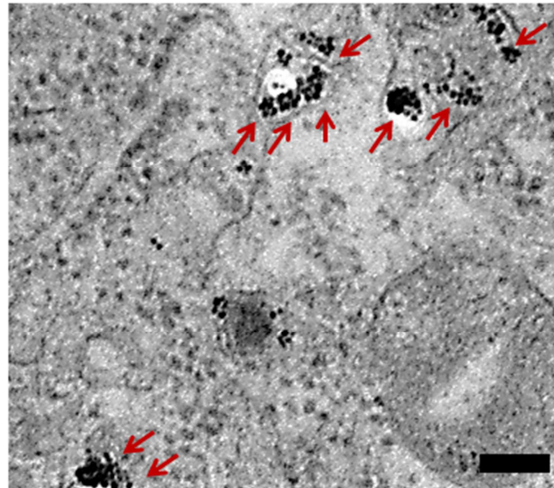
[**Figure** 4] MNCs MNC-74 cells (scale bar: 100 nm) – TEM image

In all treatments of synthesized NMCs, no more than 80% of the cell states were changed. As shown in [Figure 5], cell survival rate was high even though MNCs was injected. As a result, there was no cytotoxicity of newly synthesized MNCs.
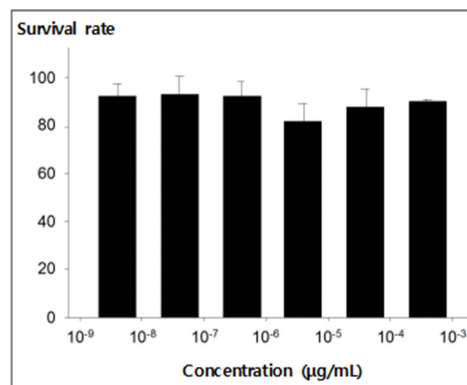
[**Figure** 5] Toxicity test results of MNC cells

[Figure 6] shows the evaluation of the degree of contrast enhancement by administering MNPs (black graph) contrast agent and clustered MNCs (gray graph) contrast agent to the cells, respectively. Comparisons of contrast enhancement after administration of the two contrast agents at the same concentration showed that the enhanced contrast enhancement effect of the clustered MNCs contrast agent was greater.
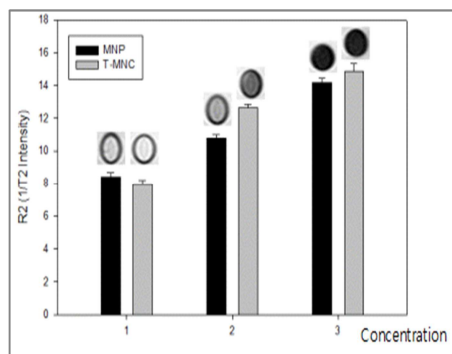
[Figure 6] Contrast enhancement of MNP and MNC

3.3. In vivo MRI

An animal model in which a gastric cancer cell line was transplanted into the thigh of a nude mouse was established. MRI was acquired using a T_2 pulse sequence after injecting the synthesized MNCs into the tail vein of a mouse. The intravenous injection into the tail vein of the nude mouse and observation of the passage of time showed that the grafted cancer cell site was specifically stressed. As shown in [Figure 7] and [Figure 8], non-MNCs images and MNCs images of cancer were acquired over time.

Over time, it was confirmed that the blood vessels in the periphery of the gastric cancer cell line were enhanced. As a result, it was found that the newly synthesized NMCs were suitable for the role of the MR molecular imaging probe for the early diagnosis of cancer.

(a) MNC-No injection   (b) MNC-Immediately after injection   (c) MNC-60 minutes after injection
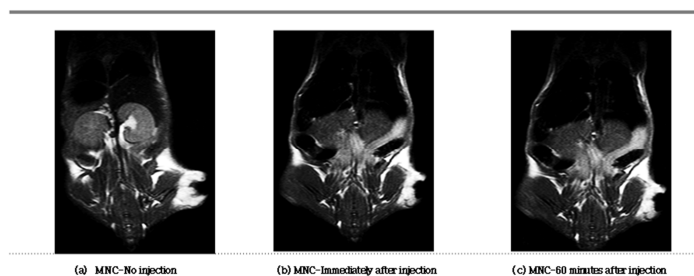
[Figure 7] Comparison of non-MNCs image and MNCs images

(a) MNC-No injection   (b) MNC-Immediately after injection   (c) MNC-60 minutes after injection
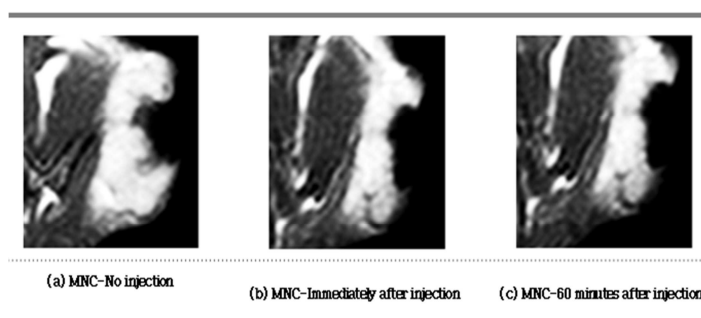
[Figure 8] Comparison between non-MNCs and MNCs images (ROI)

4. CONCLUSION

In this study, we developed molecular MR imaging nano cluster for early diagnosis of cancer.

We designed Magnetic Nanocluster is more efficient than conventional Magnetic nanoparticles in contrast enhancement issue. In addition, since magnetic nanocluster which consisting of numerous magnetic nanoparticles was synthesized with a biocompatible polymer, the toxicity issue was also resolved. In our future studies, pathological confirmation will also be required. Also, biocompatible Magnetic nanoclusters will be actively developed in clinical applications and related research.

Competing interests

The authors declare that there is no conflict of interest regarding the publication of this paper.

[REFERENCE]

[1] Pack D. S, Choi G. R, Han B. S, & Ahn, B. J.,(2012). Feature values of DWT using MR general imaging and molecular imaging. Journal of the Korean Society of Radiology, 6(5), 409-414.

[2] Nirbhay, Y.(2014). Chemical Exchange Saturation Transfer(CEST) MRI : Theory and Applications, University or Western Sydney Previous Nanoscale Research Seminars.

[3] Mahwood U.(2003), Emerging Technologies That Will Change the World, Molecular Imaging. Tech. Rev., 106.

[4] Choi, G. R., & Lee, S. B.,(2014). Application and Prospects of Molecular Imaging. J. Korean. Soc. Radiol., 8(3), 123-136.

[5] Ha S.W.(2012). Preparation and evaluation of ultrasuperparamagnetic iron oxide nanoparticle for MRI contrast agent. Mater Thesis, University of Science and Technology.

[6] Esserman, L., Wolverton, D., Hylton, N.(2002). Magnetic resonance imaging for primary breast cancer management; current role and new applications, Endo. Rel. Cancer. 9. 141.

[7] A. Maiocchi.(2003). The Use of Molecular Descriptors in the Design of Gadolinium(Ⅲ) Chelates as MRI Contrast Agents, Mini Med. Chem. 3. 845.

[8] Wang, Y., Hussain, S., & Krestin, G.,(2001). Superparamagnetic iron oxide contrast agents: physicochemical characteristics and applications in MR imaging. Eur. Radiol., 11(11). 2319-2331.

[9] Nasongkla, N., Bey, E., Ren, J., Ai, H., Khemtong, C., Guthi, J. S., Chin, S. F. Sherry, A. D., Boothman, D. A. & Gao, J.,(2006). Multifunctional Polymeric Micelles as Cancer-Targeted, MRI-Ultrasensitive Drug Delivery Systems. Nano Lett., 6(11). 2427-2430.

[10] Tournier H, Hyacinthe R, Schneider M.,(2002). Gadolinium-containing mixed micelle formulations: A new class of blood pool MRI/MRA contrast agents. Acad. Radiol. 9. S20–S28.

Blank Page

_____

Analysis of Changes in Signal Intensity of Choroidal Plexus in MRI Using FLAIR-DW-EPI Pulse Sequence

1,*Jingyu Kim, 2Sang-Jin Im

Abstract   In this study, the signal intensity of choroid plexus, which is producing cerebrospinal fluid, is analyzed according to the FLAIR diffusion-weighted imaging technique. In the T2*-DW-EPI diffusion-weighted image, the FLAIR-DW-EPI technique, which suppressed the water signal, was additionally examined for subjects with high choroid plexus signals and compared and analyzed the signal intensity. As a result of the experiment, it was confirmed that the FLAIR-DW-EPI technique showed a signal strength equal to or lower than that of the brain parenchyma, and there was a difference in signal strength between the two techniques. As a result of this study, if the choroidal plexus signal is high in the T2 * -DW-EPI diffusion-weighted image, additional examination of the FLAIR-DW-EPI technique is thought to be useful in distinguishing functional problems of the choroid plexus. In conclusion, if the choroidal plexus signal is high on the T2*-DW-EPI diffuse weighted image, it is thought that further examination of the FLAIR-DW-EPI technique will be useful in distinguishing functional problems of the choroidal plexus.

Key-word : Choroid plexuses, Diffusion weighted image, FLAIR, Signal intensity

1,*Jingyu Kim (✉) **corresponding author**
Dept. of Radiological & Madico-Oncological Science, University of Science & Technology
(34113) 217, Gajeong-ro, Yuseong-gu, Daejeon, Korea

2Sang-Jin Im
M.Sc. Biomedical Science Lee Gil Ya Cancer and Diabetes Institute, Gachon University
(21999) 155, Gaetbeol-ro, Yeonsu-ku, Incheon, Korea

I. Introduction

The diffusion-weighted image is an image of the degree of diffusion of water molecules in a tissue using an MR device[1]. The diffusion-weighted image is an image of the degree of diffusion of water molecules in a tissue using an MR device. In MRI, the diffusion of water molecules decreases the signal, so if the diffusion is good, the signal is weak, and if the diffusion is not good, the signal is strong. The clinical application of diffusion-weighted imaging is used for early diagnosis of acute cerebral infarction, differentiation between brain tumors and abscesses, and diagnosis of CJD (Creutzfeldt-Jakob Disease)[2]. Brain tissue is an aggregate of over 100 billion nerve cells, and the movement of water molecules is not completely free and is limited by the characteristics of the tissue. Isotropic diffusion refers to a case where water molecules can move in any direction, and anisotropic diffusion refers to a case where water molecules move in a specific direction only by surrounding structures[3]. Water molecules in the human brain tissue are not completely free, and in addition to the diffusion movement of fine water molecules, the movement of the brain tissue itself, cardiac movement, blood flow in the micro-vessel,

and movement of the patient are affected. The diffusion coefficient measured during actual MRI includes the effects of these various factors and is called the apparent diffusion coefficient (ADC)[4]. The degree of diffusion can be qualitatively predicted according to the signal intensity, and the diffusion coefficient can be calculated and analyzed quantitatively[5]. The choroid plexus or plica choroidea, is a plexus of cells that arises from the tela choroidea in each of the ventricles of the brain. The choroid plexus consists of modified ependymal cells surrounding a core of capillaries and loose connective tissue. There are many capillaries in the choroid layer, and consists of a window-shaped capillary and one layer of polar epithelial cells surrounding it, and is directly involved in the production of cerebrospinal fluid. The choroid plexus produces most of the cerebrospinal fluid (CSF) of the central nervous system. When the water permeability due to the difference in osmotic pressure of the choroidal plexus is significantly reduced, the production of cerebrospinal fluid is significantly reduced. MRI brain diffusion imaging has been helpful in the diagnosis and treatment of super-acute cerebral infarction in clinical practice[6]. In addition, it has been usefully used to differentiate between an arachnoid cyst and epidermoid cyst, and to diagnose brain abscess[7]. However, research on the fact that the signal intensity varies depending on the degree of diffusion according to the inspection technique of the diffusion-weighted image is not active[7]. In this study, the signal intensity of choroid plexus, which is producing cerebrospinal fluid, is analyzed according to the FLAIR diffusion-weighted imaging technique.

II. Materials and methods

1. T1 and T2 weighted image

When performing an actual MRI, 90-degree high-frequency pulses usually have to be repeatedly applied hundreds of times, so the time interval between pulses (repetition time, TR) has a great influence on the MRI signal. That is, if the TR is long, both tissues with a long T1 relaxation time or short tissues are subjected to the next 90-degree pulse while sufficiently recovering the longitudinal magnetization, and a strong signal can be generated every 90-degree pulse[8]. However, if the TR is short, the fat tissue with a short T1 relaxation time can sufficiently recover the longitudinal magnetization, but other tissues fail to recover sufficiently, and the next 90-degree pulse is applied. As a result, the MRI signal is reduced. Therefore, if the TR is shortened, an image that reflects the difference in T1 relaxation time between tissues as contrast can be created, and this is a T1 weighted image[8]. In other words, the T1 weighted image uses a short TR and a short TE, and a short TR enhances T1 contrast between tissues, and a short TE suppresses T2 contrast[8].
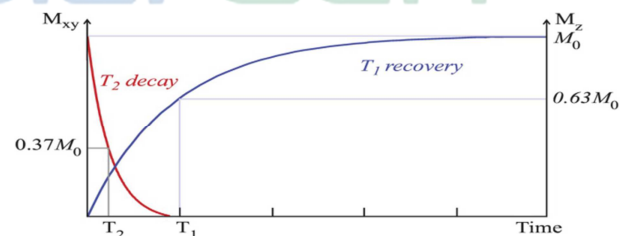
Figure 1. T1 relaxation and T2 decay[9]

The transverse magnetization created by the 90-degree high-frequency pulse decays with time. If a high-frequency pulse of 180 degrees is applied at an appropriate time, the vector of the transverse magnetization that is decaying is changed 180 degrees in the opposite direction, so that the transverse magnetization can be refocused. The time interval between the 90-degree pulse and the signal generation is called the echo time (TE), and by adjusting this, an

image reflecting the difference in T2 relaxation time between tissues as a contrast, that is, a T2 weighted image can be obtained. When TE is shortened and the transverse magnetization decay of the tissue does not occur, a 180-degree pulse is applied to obtain an image with low T2 contrast between tissues. On the other hand, when TE is lengthened and a 180-degree pulse is applied at a time when the T2 between tissues is sufficiently different, a T2 weighted image with high T2 contrast is obtained[10].
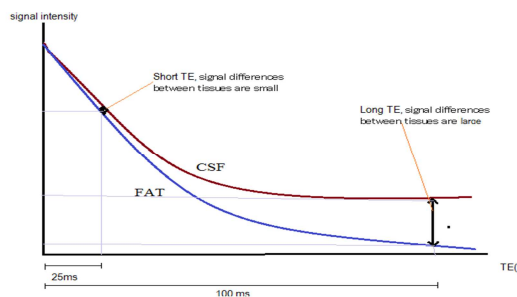

Figure 2. Signal difference between fat and water according to TE time[10]

2. FLAIR (fluid attenuated inversion recovery)

The FLAIR technique is a technique that suppresses the signals of the cerebrospinal fluid as a kind of inversion recovery technique[11]. The white matter-gray matter contrast is similar to that of the T2-weighted image, except that the signal of the cerebrospinal fluid is suppressed black because the long TR and the long TE are used. The sequence of pulses in the spin-echo image starts with a 90-degree pulse, but the inversion recovery technique applies a 180-

degree inversion pulse before the 90-degree pulse. Immediately after the 180-degree reversal pulse, the net magnetization of the tissue is completely inverted toward the (-) side of the longitudinal axis, and then T1 relaxation occurs according to the characteristics of each tissue, and magnetization in the (+) longitudinal direction begins to occur[11]. In this process, there is a point in time when the net magnetization of the vertical axis becomes zero, and the time from the 180-degree pulse to this point is called the inversion time (TI). Fat has a reversal time of 150 ms, white matter 300-400 ms, gray matter 600-700 ms, and cerebrospinal fluid 2000-2500 ms. Therefore, the 90-degree pulse is applied after waiting for the inversion time of the tissue to suppress the signal after the 180-degree inversion pulse[12]. That is, applying a 90-degree pulse after 150 ms becomes a STIR (short TI inversion recovery) technique that suppresses the fat signal, and applying a 90-degree pulse after 2000 to 2500 ms results in a FLAIR image that suppresses the cerebrospinal fluid signal. It can be seen that the signal of the desired tissue can be suppressed by adjusting the inversion time using 180-degree pulses of various inversion times while the TR and TE are fixed. FLAIR images can easily detect small lesions adjacent to the CSF space, and lesions with slightly increased T2 signals[13].
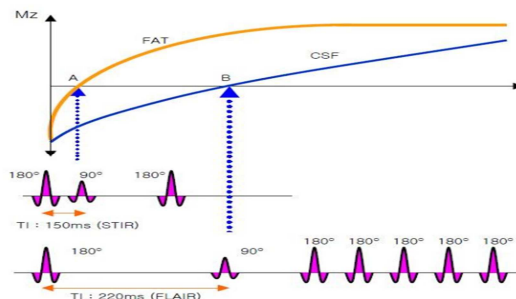
Figure 3. STIR and FLAIR according to TI[14]

Table 1. Comparison of T2 weighted images and FLAIR images[15]

	T2WI	FLAIR
Normal image		
Embolic infractions		
Acute infraction		

III. Experimental

1.5 Tesla superconducting magnetic resonance imaging device and Head & Neck coil were used. We studied 17 patients (8 males and 9 females) with the high signal intensity of choroid plexus in diffuse-weighted imaging (T2*-DW-EPI technique). An image of a subject with high signal strength with choroid plexus was additionally obtained by applying the FLAIR-DW-EPI technique. The signal intensity and diffusion coefficient of choroid plexus were obtained and compared with the diffusion-weighted images obtained by the two techniques. The parameters for obtaining diffuse-weighted images were T2*-DW-EPI and FLAIR-DW-EPI. Images were obtained using the same section of the same patient with a field of view of 28 cm, a section thickness of 6 mm, and a spacing of 1 mm. The T2*-DW-EPI technique was set to repetition time (TR) 12,000 ms, echo time (TE) 160.0 ms, and inspection time 30 sec. The FLAIR-DW-EPI technique used repetition time (TR) 12,000 ms, echo time (TE) 140.0 ms, inversion time (TI) 2,400 ms, and test time 80 sec. In order to reduce magnetic susceptibility artifacts, the lateral ventricle posterior choroid plexus was observed from the skull base to the vertex in parallel to the glabellomeatal line. For image analysis, the image data was transmitted to the Workstation, and a region of interest (ROI) at the center of the choroid plexus was designated as 28 ㎟ to obtain signal intensity and diffusion coefficient. To compare the difference between the two techniques, the signal intensity and diffusion coefficient of acute cerebral infarction and intraventricular hemorrhage were calculated.

IV. Result and Discussion

In the T2*-DW-EPI technique, 19 patients showed the high signal intensity of the choroidal plexus. Of these, 10 were male and 9 were female. The average age of all of them was 61.3 years (33~89), the average age of men was 61.5 years, and the average age of women was 59.8 years. When comparing the images examined by applying the FLAIR-DW-EPI technique to those of the T2*-DW-EPI technique, it was found that there is a significant difference in signal intensity.
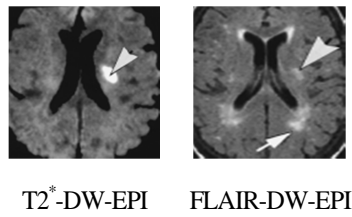
T2*-DW-EPI   FLAIR-DW-EPI

Figure 4. Choroid plexus

Quantitatively, in the T2*-DW-EPI technique, the signal intensity of the choroid plexus was 251.6 ㎟/s and the apparent diffusion coefficient (ADC) was 1.86×103 ㎟/s. The FLAIR-DW-EPI technique was 61.3 ㎟/s and the ADC was 1.84×103 ㎟/s, which was similar to the brain cortex. The difference in signal intensity between the two techniques was 191 ㎟, which was highly observed in the T2*-DW-EPI technique, and there was little difference in the overt diffusion coefficient. In the case of acute cerebral infarction, both techniques showed high signal intensity and were 251.5 ㎟/s and 212.8 ㎟/s, respectively, and ADCs were 0.81×103 ㎟/s and 0.80×103 ㎟/s, respectively.
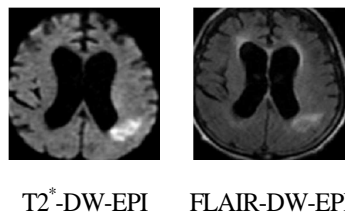

T2*-DW-EPI   FLAIR-DW-EPI

Figure 5. Acute cerebral infarction

Table 2. Signal intensity analysis

Label	DW-EPI	Signal intensity	ADC(X10³)
Brain	T2*	116.1	1.08
	FLAIR	113.1	1.23
Choroid plexus	T2*	250.8	1.87
	FLAIR	60.8	1.85

Acute infraction	T2*	250.5	0.82
	FLAIR	212.6	0.80
Acute hemorrhage	T2*	389.4	0.84
	FLAIR	337.6	0.76

In the case of a lateral ventricular cerebral hemorrhage, both techniques showed high signal intensity, 389.6 ㎟/s, and 337.8 ㎟/s, respectively, and ADCs were 0.83×103 ㎟/s and 0.77×103 ㎟/s, respectively.
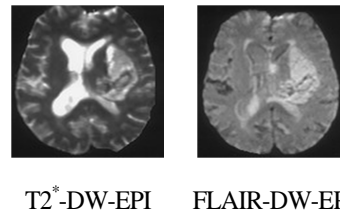

T2*-DW-EPI   FLAIR-DW-EPI

Figure 6. Lateral ventricular cerebral hemorrhage

The degree of signal attenuation by diffusion is proportional to the moving size of the molecule and the intensity of the diffusion-enhanced gradient magnetic field. The intensity of the diffusion-enhanced gradient magnetic field is called b-value (s/㎟), which is related to the intensity of the gradient magnetic field, the time applied to the gradient magnetic field, and the time interval between the front and rear gradient magnetic fields. In general, diffuse-enhanced images can be sufficiently visualized by applying a b value of about 1,000. In the diffusion-weighted image, the signal intensity is determined by the combination of the overt diffusion coefficient and the T2 component, which indicates the degree of diffusion of water molecules in the tissue. If the b value is 0s / ㎟, the T2 weighted image is displayed, and you can increase the B value to reduce the T2 effect or suppress the water signal[15].

In this study, the diffusion gradient magnetic field was applied in the selection direction of the section, the frequency

coding direction, and the phase coding direction. T2*-DW-EPI technique with b-value (s/㎟) of 1,000 and the resonant frequency is applied by setting the null point as the inversion time when the water molecule signal reaches the x, y plane A FLAIR-DW-EPI technique was used to obtain the results of the spread and signal intensity of choroid plexus. Most of choroid plexus did not show high signal intensity in T2*-DW-EPI testers, but showed the same or low signal intensity as the brain parenchyma. The subjects of this study were tested with subjects with high signal strength. As a result of comparing the signal and diffusion degree of choroid plexus between the two techniques, the T2*-DW-EPI technique showed high signal strength. On the other hand, the FLAIR-DW-EPI technique, which suppressed the water signal, showed the same or low signal intensity as that of the brain parenchyma and was compared. However, there was no difference in the overt diffusion coefficient. Choroid plexus is considered to exhibit high signal strength as the T2 effect remains in the T2*-DW-EPI technique. Due to the structure of the choroid plexus, the process of generating cerebrospinal fluid in countless capillaries was partially transformed into a sponge-type cystic structure, and it is believed that the diffusion of water molecules was slower than that of stagnant or normal people, resulting in high signal intensity[16]. In the results of the FLAIR-DW-EPI test, which suppressed the water signal, the sponge-type cystic structure showed a signal similar to or lower than that of the brain parenchyma as the water signal was suppressed. On the other hand, in the case of acute cerebral infarction and acute cerebral hemorrhage, both techniques showed high signal intensity.

V. Conclusion

In this study, the signal intensity of the choroid plexus generating cerebrospinal fluid was analyzed by acquiring signals using the T2*-DW-EPI technique and the FLAIR-DW-EPI technique. Acute cerebral infarction and acute cerebral hemorrhage on diffuse-weighted images were observed with higher signal intensity compared to normal brain in diffuse images, and the overt diffusivity (ADC) was observed to be low, confirming that it is an excellent technique for diagnosing acute cerebral infarction. In the T2*-DW-EPI diffusion-weighted image, the FLAIR-DW-EPI technique, which suppressed the water signal, was additionally examined for subjects with high choroid plexus signals and compared and analyzed the signal intensity. As a result, it was confirmed that the FLAIR-DW-EPI technique showed a signal intensity equal to or lower than that of the brain parenchyma, and there was a difference in signal intensity between the two techniques. The results of this study are that in patients with high choroid plexus signals on T2*-DW-EPI diffusion-weighted images, the FLAIR-DW-EPI technique was additionally examined. It is thought to be useful for the discrimination of cystic structures.

[Reference]

[1] Mukherji, Suresh K, Chenevert, Thomas L, Castillo, Mauricio, "*Diffusion-Weighted Magnetic Resonance Imaging*", Journal of Neuro-Ophthalmology, Vol. 22, Issue 2, PP. 118~122(2002)

[2] Pamela W. Schaefer, P. Ellen Grant, R. Gilberto Gonzalez, "*Diffusion-weighted MR Imaging of the Brain*", Radiology, RSNA 2000 ; 217:331~345(2000)

[3] Yong Sang, Jingfeng Xu, "*Evaluation of Motor Neuron Injury in ALS by Different Parameters of Diffusion Tensor Imaging*", IEEE Access, Vol. 8, pp. 72381~72394(2020)

[4] Bhupesh Sharma, Kanishk Luhach, G. T. Kulkarni, "*4-In vitro and in vivo models of BBB to evaluate brain targeting drug delivery*", Brain Targeted Drug Delivery System, pp. 53~101(2019)

[5] Maarten G. Lansberg, Vincent N. Thijs, Michael W. O'Brien, Juan O. Ali, et al., "*Evolution of Apparent Diffusion Coefficient, Diffusion-weighted, and T2-weighted Signal Intensity of Acute Stroke*", AJNR, Vol. 22, No. 4, pp. 637~633(2001)

[6] Matthew J. Tait, Samira Saadoun, B. Anthony Bell, Marios C. Papadopoulos, "*Water movements in the brain: role of aquaporins*", Trends in Neurosciences, Vol. 31, Issue 1, pp. 37~43(2008)

[7] David John Werring, "*Mechanisms of central nervous system damage and recovery in demyelinating and other neurological disorders: structural and functional MRI studies*", Doctoral dissertation, University College London, ProQuest LLC(2016)

[8] Gary D. Fullerton, "*Magnetic Resonance Imaging Signal Concept*", RadioGraphics, Vol. 7, No. 3, PP. 579~596(1987)

[9] McRobbie, D., Moore, E., Graves, M., & Prince, M. (2017). "*Getting in Tune: Resonance and Relaxation. In MRI from Picture to Proton* "(pp. 124-143). Cambridge: Cambridge University Press. doi:10.1017/9781107706958.010

[10] *https://mrimaster.com/characterise%20physics.html* (04-22-2020)

[11] R. Kates, D. Atkinson, M. Brant-Zawadzki, "*Fluid-attenuated inversion recovery(FLAIR): clinical prospectus of current and future applications*", Top Magn Reson Imaging, Vol. 8, No. 6, PP. 389~396(1996)

[12] http://radiopaedia.org (04-26-2020),"*Double inversion recovery sequence*", rID : 32070 (04-26-2020)

[13] Filippo Del Grande, Francesco Santini, Daniel A. Herzka, et al., "*Fat-Suppression Technique for 3-T MR Imaging of the Musculoskeletal System*", Radiographics, Vol. 34, No. 1, pp. 217~233(2014)

[14] *http://www.researchgate.net/figure/Comparison-of-conventional-and-Synthetic-Contrast-MRI-T2-weighted-FLAIR_fig6_308038621* (04-08-2020)

[15] Dmitriy A. Yablonskiy, Alexander L. Sukstanskii, "*Theoretical models of the diffusion weighted MR signal*", Published online in Wiley Online Library: 3 June 2010, pp. 661~681(2010), DOI:10.1002/nbm.1520

[16] Melody P. Lun, Edwin S. Monuki, Maria K. Lehtinen, "*Development and functions of the choroid plexus-cerebrospinal fluid system*", Nat Rev Nuerosci, Vol. 16, No. 8, pp. 445~457(2015)

Blank Page